Computational study on ammonia adsorption on the $X_{12}Y_{12}$ nano-clusters (X = B, Al and Y = N, P)

Ali Ahmadi Peyghan[1,*] and Hamed Soleymanabadi[2]

[1]Young Researchers and Elite Club, Central Tehran Branch, Islamic Azad University, Tehran, Iran
[2]Department of Chemistry, College of Science, Central Tehran Branch, Islamic Azad University, Tehran, Iran

The adsorption of ammonia (NH_3) on four $X_{12}Y_{12}$ (X = B, Al and Y = N, P) nano-cages was investigated using density functional theory calculations. Changes in Gibbs free energy, adsorption energy, frequency modes, natural bond orbitals, molecular electrostatic potential surfaces and density of states were explored. It was found that the relative order of the acidity for the surfaces is: $Al_{12}N_{12} > Al_{12}P_{12} > B_{12}N_{12} > B_{12}P_{12}$. In the case of $Al_{12}N_{12}$, hybridization and lower electron density of the adsorbing atom overcome the disadvantage of high HOMO–LUMO (highest occupied molecular orbital–lowest unoccupied molecular orbital) energy gap (E_g); therefore, this cage becomes the most favourable for the adsorption of NH_3. We found that changes in the electronic properties of the clusters are negligible after the adsorption process. Also, the value of E_g increases with the increase in the Hartree–Fock exchange per cent of the density functional.

Keywords: Acidity of surfaces, ammonia adsorption, density functional theory, nano-clusters.

SURFACE acidity is an important property that is frequently used to characterize the reactivity of surfaces. Ammonia (NH_3) is widely used as a probe molecule to experimentally determine the Lewis and Brønsted acidity of surfaces, and the binding energy to a particular site on the surface serves as a measure of its acid strength[1]. Most surfaces have several types of reactive sites, and with the addition of a dopant, the number of such sites can increase further[2]. Theoretical methods are well suited to numerically probe the strength of the binding of NH_3 to the numerous reactive sites, and provide rich information about the reactivity of the surface[3,4].

During the last decade, fullerene-related materials have attracted considerable attention because of their unique physical and chemical properties[5–12]. In the theoretical studies on several $(XY)_n$ clusters, the fullerene-like cages $X_{12}Y_{12}$ were predicted to be the most stable ones[13,14]. These facts show that the fullerene-like cage $(XY)_n$ may be a desired cluster and has inherent special stability when $n = 12$. Jensen and Toftlund[15] carried out *ab initio* quantum chemical calculations on $B_{12}N_{12}$ with various geometries. They found that $B_{12}N_{12}$ fullerenes are characterized by higher stability than C_{24}, provided that they have four- and six-membered rings (MRs), but without so-called 'erroneous' BB and NN bonds. Oku *et al.*[16] have synthesized the $B_{12}N_{12}$ detected by laser desorption time-of-flight mass spectrometry.

Recently, theoretical investigations have been made which address the stability of aluminium nitride nanostructures based on *ab initio* calculations[17]. The structure and stability of fullerene-like cages of $(AlN)_n$ ($n = 2$–41) were studied. It was suggested that $(AlN)_{12}$ is energetically the most stable cluster in this family and would thus be an ideal inorganic fullerene-like cage. Because of sp^2 hybridization of metal–nitrogen bonds, these graphitic-like layered cluster structures were found to be energetically stable. AlP clusters are prominent targets of study because of their higher vibrational frequencies and facilitating ability of the observation of vibrational progression in photoelectron spectra. Additionally, the smaller number of electrons makes them more amenable to electronic structure calculations. To date, several *ab initio* calculations have been carried out on the properties of Al_nP_m clusters by several groups[18–20].

Boron phosphide (BP) four- and six-MRs have been made available previously[21]. Boron phosphide is a refractory semiconductor compound with peculiar properties. It is a III–V material with a strong covalent binding character; its zinc blende structural phase is the most stable, and it is a promising material for application in optoelectronic and microelectronic devices working under difficult conditions such as high temperature or aggressive environment[22]. Here, we present a comparative study on the acidity of $B_{12}N_{12}$, $Al_{12}N_{12}$, $B_{12}P_{12}$ and $Al_{12}P_{12}$ nano-clusters by means of density functional theory (DFT) calculations.

We selected four fullerene-like $X_{12}Y_{12}$ (X = B, Al and Y = N, P) nano-clusters, optimized parameters of which are shown in Figure 1. Structure optimization, frontier molecular orbitals (FMOs), natural bond orbitals (NBOs), and molecular electrostatic potential (MEP) analyses were performed using three-parameter hybrid generalized gradient approximation B3LYP functional augmented with an empirical dispersion term (B3LYP-D) with 6-31G basis set, including the d-polarization function (denoted as 6-31G (d)) as implemented in the GAMESS suite of programs[23]. GaussSum program was used to obtain density of states (DOS) results[24]. The B3LYP, a combination of Hartree–Fock (HF) with a DFT based on the Becke three-parameter exchange coupled with the Lee–Yang–Parr (LYP) correlation potential[25], is one of the most popular hybrid density functional methods. Previously, it has been shown that the geometry structure of fullerene (C_{60}) predicted by B3LYP calculations is in good agreement with the experiments[26]. The B3LYP was demonstrated to be a reliable functional, and it is commonly used in the study of different nano-structures[27–31]. Vibration frequencies were calculated at the same level of

*For correspondence. (e-mail: ahmadi.iau@gmail.com)

theory to confirm that all of the stationary points correspond to a true minima on the potential energy surface. All frequency calculations were performed using numerical second derivatives and it was verified that all of the structures are true minima according to frequency analysis and all positive Hessian eigenvalues obtained. We have defined the adsorption energy (E_{ad}) as follows

$$E_{ad} = E(NH_3/X_{12}Y_{12}) - E(X_{12}Y_{12}) - E(NH_3) + E(\text{BSSE}), \quad (1)$$

where E ($NH_3/X_{12}Y_{12}$) is the total energy of the NH_3 molecule adsorbed on the $X_{12}Y_{12}$ surface, and E ($X_{12}Y_{12}$) and E (NH_3) are the total energies of the pristine $X_{12}Y_{12}$, and NH_3 molecule respectively. E (BSSE) is the basis set superposition error (BSSE) corrected for all interaction energies. According to the definition, negative values of E_{ad} correspond to the exothermic process.

The optimized structures of the title nano-clusters with the geometrical parameters are shown in Figure 1. A significant difference between the XY fullerenes and the carbon fullerenes is that the former are comprised of two different atoms. Generally, a $X_{12}Y_{12}$ nano-cage is formed from eight 6-MRs and six 4-MRs with T_h symmetry, so that the calculated electric dipole moment is zero. The computed NMR spectra of all clusters consist of two single peaks, in agreement with their T_h symmetry. Structurally, there are two types of individual X–Y bonds among 36 X–Y bonds in $X_{12}Y_{12}$; one is shared by two 6-MRs (B_{66}), and the other by 4- and 6-MRs (B_{64}). The B_{64} bonds are slightly longer than the B_{66} bonds. The lengths of these bonds are equal to those obtained by Beheshtian *et al.*[32].

To find the most stable NH_3-adsorbed configuration, several distinct starting structures were used for optimization, including N or H head located on the top of X or Y atom of the cluster surfaces and parallel or on-bridge configurations. As shown in Figure 2, the most stable configuration is that in which the N atom of NH_3 is close to the X atom of the clusters. The adsorption of NH_3 on the X site (B or Al) of the clusters can be clearly rationalized by the fact that in $X_{12}Y_{12}$, highest occupied molecular orbital (HOMO) is localized on the Y atoms, and lowest unoccupied molecular orbital (LUMO) is located on the X atoms. As a result, ammonia (Lewis base which acts as a probe molecule to determine the acidity of surfaces experimentally) is adsorbed strongly on Lewis acid sites (X site). In the most stable configurations of NH_3 adsorbed on AlN, BP, AlP and BN clusters, the interaction distances between the N atom of NH_3 and the X atoms are 2.03, 1.64, 2.06, and 1.63 Å, and the E_{ad} values are –37.5, –27.0, –32.8 and –29.8 kcal/mol respectively (Table 1). Furthermore, the NH_3 adsorption induces a

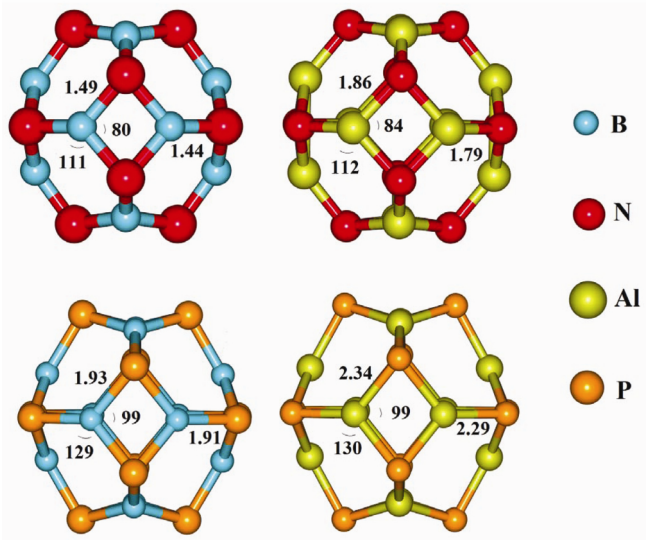

Figure 1. Geometrical parameters of optimized structures of $B_{12}N_{12}$, $Al_{12}N_{12}$, $B_{12}P_{12}$ and $Al_{12}P_{12}$ inorganic fullerene-like cages. Distances and angels are in angstrom and degree respectively.

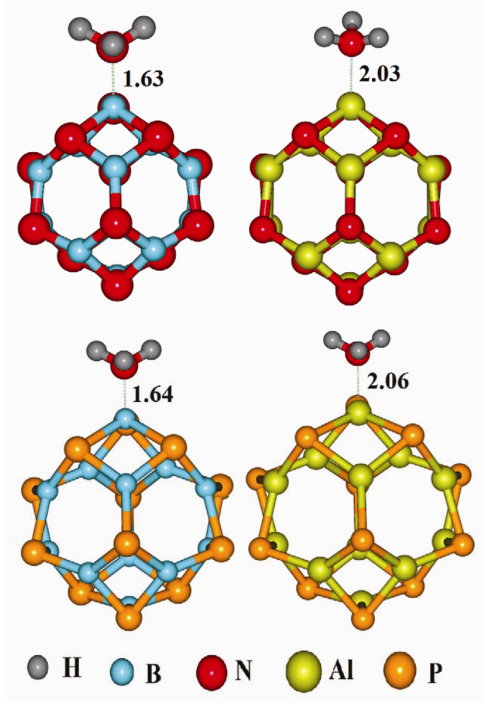

Figure 2. Structure of optimized $NH_3/X_{12}Y_{12}$ (bonds in Å).

Table 1. Calculated energies (kcal/mol) of NH_3 adsorption with the clusters studied (E_{ad}, ΔG and ΔH)

System	E_{ad}	ΔG	ΔH	[a]Q_T (e)
$B_{12}N_{12}$	–			–
$NH_3/B_{12}N_{12}$	–29.8	–25.6	–23.3	0.418
$Al_{12}N_{12}$	–			–
$NH_3/Al_{12}N_{12}$	–37.5	–33.4	–29.8	0.333
$B_{12}P_{12}$	–			–
$NH_3/B_{12}P_{12}$	–27.0	–22.9	–19.1	0.534
$Al_{12}P_{12}$	–			–
$NH_3/Al_{12}P_{12}$	–32.8	–28.7	–25.0	0.611

[a]Q_T is defined as the total charge on NH_3.

locally structural deformation to both the NH_3 molecule and the clusters. To explore the effect of entropy on the adsorption processes, change of Gibbs free energies (ΔG) was calculated at standard temperature and pressure (1 atm and 298 K respectively), applying the same level which was used for the optimization. The results (Table 1) indicate that ΔG values are somewhat less negative than those of E_{ad} because of the entropic effect. However, the energetic favourability of NH_3 adsorption on the studied clusters is in order AlN > AlP > BN > BP.

It is known that one of the most important factors in interactions is the kinetic stability (an index of the reactivity of molecules[33]) of the clusters. There is a direct relationship between the stability and HOMO–LUMO energy gap (E_g) of the clusters, i.e. greater E_g leads to more stability[33]. To gain an accurate E_g for every nano-cluster studied, we applied different DFT functionals, including B3LYP, X3LYP and M06 combined with the 6-31G (d) basis sets. The calculated results are summarized in Table 2, indicating that the E_g values are dependent on the functional types. The B3LYP and M06 yield the smallest and the largest values respectively. It can be seen that by increasing the HF exchange percentage of density functionals the predicted E_g becomes larger. The HF exchange percentage is about 20.0, 21.8 and 27.4 for B3LYP, X3LYP and M06 respectively. Since there are no experimental data for E_g, we calculated the average value of the results for these functionals. The relative order magnitudes of E_g (eV) are as follows

$$B_{12}N_{12}\ (7.09) >> Al_{12}N_{12}\ (4.12) > B_{12}P_{12}\ (3.87) > Al_{12}P_{12}\ (3.49).$$

The $Al_{12}P_{12}$ nano-cluster has the smallest E_g; therefore, it is the most electrically conductive cluster. The $B_{12}N_{12}$ case has the most electrical resistivity because of the largest E_g. All the above suggest that the $B_{12}N_{12}$ nano-cluster is an insulator material, but the others are semiconductors. There is a definite correlation between the size of atoms and E_g of the clusters, i.e. the clusters that consist of atoms with greater covalent radius have smaller E_g. This can be rationalized by the fact that larger atoms have higher polarizability and their valence electrons can freely contribute to the electrical conductivity. The absolute values of E_g may be an appropriate factor to compare the kinetic stability of these clusters because the number of atoms in all clusters is equal. As a result, their relative kinetic stability is $B_{12}N_{12} > Al_{12}N_{12} > B_{12}P_{12} > Al_{12}P_{12}$, which does not support the corresponding E_{ad}. Therefore, we seek other parameters to explain this phenomenon.

Table 2. HOMO–LUMO gap (E_g; in eV) of the $B_{12}N_{12}$, $Al_{12}N_{12}$, $B_{12}P_{12}$ and $Al_{12}P_{12}$ clusters calculated using different density functional theory functionals

Cluster	B3LYP	X3LYP	M06	Mean
$B_{12}N_{12}$	6.84	6.97	7.47	7.09
$Al_{12}N_{12}$	3.93	4.05	4.39	4.12
$B_{12}P_{12}$	3.71	3.79	4.12	3.87
$Al_{12}P_{12}$	3.39	3.48	3.61	3.49

The equilibrium bond lengths of X–Y for BN, AlN, BP and AlP cages are shown in Table 3. It can be found that both of them are shorter than the single bond in H_3X–YH_3, but longer than the double bond in H_2X–PY_2 at spin-unrestricted B3LYP/6-31G (d). This indicates that the $X_{12}Y_{12}$ clusters have aromatic nature stabilized by the p electron conjugation. NBO analysis shows that the adsorption of NH_3 on the clusters needs a rehybridization of adsorbing atoms so that the p-character is increased. Therefore, the atoms whose hybridization has more p-character may able to adsorb the NH_3 molecule easily with a low structure deformation. Although, based on NBO analysis, the hybridization of electron-rich P and N atoms is nearly sp^3 and sp^2 respectively, all adsorbing X atoms have nearly sp^2 hybridization. Hence, we conclude that this factor cannot affect the E_{ad} values.

We have shown that the strong interaction between the NH_3 molecule and AlN nano-tubes is mainly electrostatic rather than covalent because of the high heteropolar nature of Al–N bonds[34]. The Mulliken (and NBO) charges transferred from the electropositive atom (X) to electronegative atom (Y) on the surfaces of $B_{12}N_{12}$, $Al_{12}N_{12}$, $B_{12}P_{12}$ and $Al_{12}P_{12}$ clusters are 0.44 (1.17), 0.74 (1.85), 0.19 (0.28) and 0.21 (1.10) *e* respectively. The ionicity of the Al–N and B–N bonds is significantly more than that of both B–P and Al–P bonds. We have shown the MEP plots for the all clusters, confirming that the highest electron transfer from the electropositive atom (X) to the electronegative atom (Y) occurs on the surface of $Al_{12}N_{12}$. As shown in Figure 3 on the surface of $Al_{12}N_{12}$, Al and N atoms are intensively blue (positive charge) and red (negative charge) respectively, whereas the colour separation is very low on the surface of $B_{12}P_{12}$, because of less charge transfer from B to P atoms. It can

Table 3. Lengths of B_{64} and B_{66} bonds on the surface of $X_{12}Y_{12}$ clusters in comparison with those of H_3X–YH_3 and H_2X–YH_2

Cluster	B_{66}	B_{46}	H_3X–YH_3	H_2X–YH_2
$B_{12}N_{12}$	1.44	1.49	1.36	1.69
$Al_{12}N_{12}$	1.79	1.89	1.71	1.99
$B_{12}P_{12}$	1.91	1.93	1.85	1.99
$Al_{12}P_{12}$	2.30	2.34	2.32	2.58

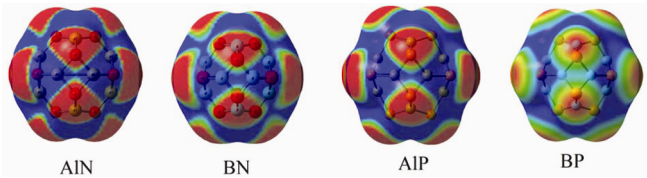

Figure 3. Molecular electrostatic potential surfaces for $X_{12}Y_{12}$. Colour range (in arb. units): –0.01 (red), + 0.01 (blue).

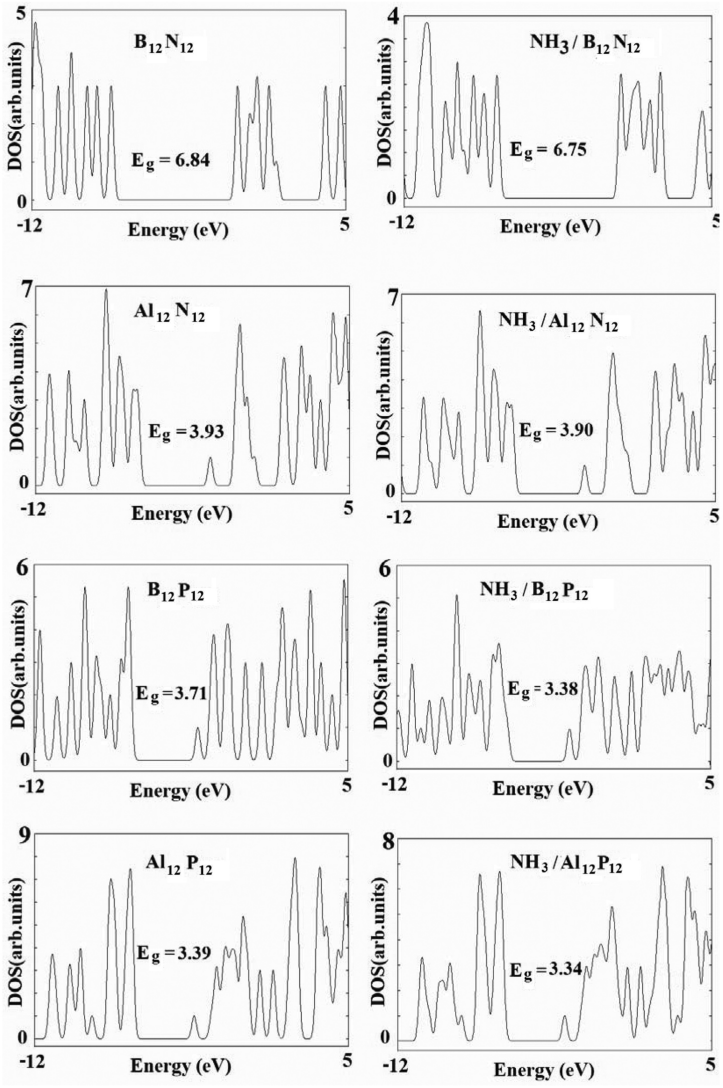

Figure 4. Density of states (DOS) plots of pristine and NH_3 adsorbed $X_{12}Y_{12}$.

be concluded that the electron-rich N atom of the NH_3 molecule strongly tends to interact with the electron-poor Al atoms of $Al_{12}N_{12}$ and this may result in more negative value of E_{ad}.

On the other hand, as we have mentioned above, NBO analysis shows that during the strong adsorption of NH_3 on the cluster surface, the adsorbing atom tends to attain sp^3 hybridization. However, this rehybridization from sp^2 to sp^3 can be simplified by flexible long bonds around the adsorbing atoms. In the case of $B_{12}N_{12}$, shorter B–N bonds around the B atom (adsorbing site) strongly avoid the rehybridization of B atoms from sp^2 to sp^3 after the adsorption process. As a result, the adsorption of NH_3 molecule on $B_{12}N_{12}$ is severely suppressed by $Al_{12}N_{12}$. Thus, in the case of $Al_{12}N_{12}$ hybridization and lower electron density of the adsorbing atom overcome the disadvantage of more negative E_g, as this case becomes the most favourable to NH_3 adsorption. Despite the relatively low kinetic stability, and E_g, in both $Al_{12}P_{12}$, and $B_{12}P_{12}$, less p-character and higher electron density of X atoms lead to smaller E_{ad} values. In the case of BN, despite the partly low electron density of the adsorbing atom (B), one disadvantage (the shorter bond lengths) leads to lower E_{ad} than in $Al_{12}N_{12}$ and $Al_{12}P_{12}$. However, the relative order magnitudes of acidity strength are $Al_{12}N_{12} > Al_{12}P_{12} > B_{12}N_{12} > B_{12}P_{12}$.

Finally, we have studied the influence of NH_3 adsorption on the electronic properties of the clusters. The nature of the DOS cluster near the Fermi level is critical to the understanding of electrical transport through these materials. Therefore, we have drawn DOS plots for $X_{12}Y_{12}$ with and without NH_3 through B3LYP/6-31G (d) level of theory (Figure 4). Although conduction and valence levels shift to lower energies after the adsorption of NH_3 in the all clusters, the E_g of $B_{12}N_{12}$, $Al_{12}N_{12}$, $B_{12}P_{12}$ and $Al_{12}P_{12}$ clusters decreases slightly by 0.09, 0.33, 0.03 and 0.05 eV respectively. These changes in electronic properties are negligible, indicating that the

electronic properties of clusters are insensitive to the NH_3 molecule. The calculated DOS show that NH_3 adsorption on $X_{12}Y_{12}$ (X = B, Al and Y = N, P) cages can be generally classified as a certain type of 'electronically harmless modification'.

The adsorption of the NH_3 molecule was investigated on the $B_{12}N_{12}$, $Al_{12}N_{12}$, $B_{12}P_{12}$ and $Al_{12}P_{12}$ nano-cages employing DFT calculations. It was found that NH_3 prefers to be adsorbed on a B or Al atom of the clusters, releasing energy in the range 27.0–37.5 kcal/mol. Relative order of the acidity for different surfaces is: $Al_{12}N_{12} > Al_{12}P_{12} > B_{12}N_{12} > B_{12}P_{12}$. It was found that the energetic feasibility of this process depends on several factors such as the electron density and length of the surrounding bonds of the adsorbing atoms and their hybridization. These factors compete with each other in determining the adsorption behaviour of the nano-cages. Molecular electrostatic potential and NBO analyses show that the high polar surface and large bond lengths of cluster surfaces are conducive to the adsorption of NH_3 on $Al_{12}N_{12}$ cluster.

1. Yao, H., Chen, Y., Wei, Y., Zhao, Z., Liu, Z. and Xu, C., A periodic DFT study of ammonia adsorption on the $V_2O_5(001)$, $V_2O_5(010)$ and $V_2O_5(100)$ surfaces: Lewis versus Brönsted acid sites. *Surf. Sci*., 2012, **606**, 1739–1748.
2. Joshi, A., Rammohan, A., Jiang, Y. and Ogunwumi, S., Density functional theory (DFT) study of the interaction of ammonia with pure and tungsten-doped ceria. *J. Mol. Struct.: THEOCHEM*, 2009, **912**, 73–81.
3. Onal, I., Soyer, S. and Senkan, S., Adsorption of water and ammonia on TiO_2-anatase cluster models. *Surf. Sci*., 2006, **600**, 2457–2469.
4. Elanany, M., Koyama, M., Kubo, M., Broclawik, E. and Miyamoto, A., Periodic density functional investigation of Lewis acid sites in zeolites: relative strength order as revealed from NH_3 adsorption. *Appl. Surf. Sci*., 2005, **246**, 96–101.
5. Kroto, W., Heath, J. R., O'Brien, S. C., Curl, R. F. and Smalley, R. E., C60: Buckminsterfullerene. *Nature*, 1985, **318**, 162–163.
6. Jemmis, E. D. and Manoharan, M., Strategies to stabilize exohedral η5- and η6-fullerene transition metal organometallic complexes: a molecular orbital treatment. *Curr. Sci*., 1999, **76**, 1122–1126.
7. Srinivasan, C., From fullerene-C60 to four-wheelers. *Curr. Sci*., 2006, **91**, 580–582.
8. Abhijith Kumar, R. P. S., Dev, S., Mishra, B. K. and Sathyamurthy, N., Stabilization of the C_{20} cage by encapsulation of H^+ and He^{2+} ions. *Curr. Sci*., 2014, **106**, 1255–1259.
9. Beheshtian, J., Bagheri, Z., Kamfiroozi, M. and Ahmadi, A., Toxic CO detection by $B_{12}N_{12}$ nanocluster. *Microelectron. J*., 2011, **42**, 1400–1403.
10. Beheshtian, J., Kamfiroozi, M., Bagheri, Z. and Peyghan, A. A., $B_{12}N_{12}$ nano-cage as potential sensor for NO_2 detection. *Chin. J. Chem. Phys*., 2012, **25**, 60–64.
11. Beheshtian, J., Peyghan, A. A. and Bagheri, Z., Adsorption and dissociation of Cl_2 molecule on ZnO nanocluster. *Appl. Surf. Sci.*, 2012, **258**, 8171–8176.
12. Moradi, M., Peyghan, A. A., Bagheri, Z. and Kamfiroozi, M., Cation–π interaction of alkali metal ions with C 24 fullerene: a DFT study. *J. Mol. Model*., 2012, **18**, 3535–3540.
13. Strout, D. L., Structure and stability of boron nitrides: isomers of $B_{12}N_{12}$. *J. Phys. Chem. A*, 2000, **104**, 3364–3366.
14. Wang, R., Zhang, D. and Liu, C., Theoretical prediction of a novel inorganic fullerene-like family of silicon–carbon materials. *Chem. Phys. Lett.*, 2005, **411**, 333–338.
15. Jensen, F. and Toftlund, H., Structure and stability of C_{24} and $B_{12}N_{12}$ isomers. *Chem. Phys. Lett*., 1993, **201**, 89–96.
16. Oku, T., Nishiwaki, A. and Narita, I., Formation and atomic structure of $B_{12}N_{12}$ nanocage clusters studied by mass spectrometry and cluster calculation. *Sci. Technol. Adv. Mater*., 2004, **5**, 635–645.
17. Wu, H. S., Zhang, F. Q., Xu, X. H., Zhang, C. J. and Jiao, H., Geometric and energetic aspects of aluminum nitride cages. *J. Phys. Chem. A*, 2003, **107**, 204–209.
18. Feng, P. Y. and Balasubramanian, K., Spectroscopic properties of Al_2P_2, $Al_2P_2^+$, and $Al_2P_2^-$ and comparison with their Ga and in analogues. *J. Phys. Chem. A*, 1999, **103**, 9093–9099.
19. Archibong, E. F., Gregorius, R. M. and Alexander, S. A., Structures and electron detachment energies of AlP_2^- and Al_2P_2. *Chem. Phys. Lett*., 2000, **321**, 253–261.
20. Feng, P. Y. and Balasubramanian, K., Potential energy surfaces of electronic states of AlP_2, Al_2P and their ions. *Chem. Phys. Lett*., 2000, **318**, 417–426.
21. Pestana, D. C. and Power, P. P., Nature of the boron–phosphorus bond in monomeric phosphinoboranes and related compounds. *J. Am. Chem. Soc*., 1991, **113**, 8426–8437.
22. Ferreira, V. and Alves, H., Boron phosphide as the buffer-layer for the epitaxial III-nitride growth: a theoretical study. *J. Crystal Growth*, 2008, **310**, 3973–3978.
23. Schmidt, M. W. *et al.*, General atomic and molecular electronic structure system. *J. Comput. Chem*., 1993, **14**, 1347–1363.
24. O'Boyle, N., Tenderholt, A. and Langner, K., cclib: A library for package-independent computational chemistry algorithms. *J. Comput. Chem*., 2008, **29**, 839–845.
25. Lee, C., Yang, W. and Parr, R. G., Development of the Colle–Salvetti correlation-energy formula into a functional of the electron density. *Phys. Rev. B*, 1988, **37**, 785–789.
26. Hu, Y. and Ruckenstein, E., *Ab initio* quantum chemical calculations for fullerene cages with large holes. *J. Chem. Phys*., 2003, **119**, 10073–10080.
27. Peyghan, A. A. and Noei, M., Hydrogen fluoride on the pristine, Al and Si doped BC_2N nanotubes: a computational study. *Comput. Mater. Sci.*, 2014, **82**, 197–201.
28. Kakemam, J. and Peyghan, A. A., Electronic, energetic, and structural properties of C- and Si-doped $Mg_{12}O_{12}$ nano-cages. *Comput. Mater. Sci*., 2013, **79**, 352–355.
29. Kökten, H. and Erkoç, S., Energetics and structural properties of carbon and oxygen doped hexagonal boron nitride sheets. *Physica E*, 2011, **44**, 215–217.
30. Beheshtian, J., Peyghan, A. A. and Bagheri, Z., Selective function of $Al_{12}N_{12}$ nano-cage towards NO and CO molecules. *Comput. Mater. Sci*., 2012, **62**, 71–74.
31. Beheshtian, J., Kamfiroozi, M., Bagheri, Z. and Ahmadi, A., Theoretical study of hydrogen adsorption on the $B_{12}P_{12}$ fullerene-like nanocluster. *Comput. Mater. Sci*., 2012, **54**, 115–118.
32. Beheshtian, J., Bagheri, Z., Kamifiroozi, M. and Ahmadi, A., A comparative study on the $B_{12}N_{12}$, $Al_{12}N_{12}$, $B_{12}P1_2$ and $A_{l2}P_{12}$ fullerene-like cages. *J. Mol. Model*., 2012, **18**, 2653–2658.
33. Yoshida, M. and Aihara, J., Validity of the weighted HOMO–LUMO energy separation as an index of kinetic stability for fullerenes with up to 120 carbon atoms. *Phys. Chem. Chem. Phys*., 1999, **1**, 227–230.
34. Ahmadi, A., Beheshtian, J. and Hadipour, N. L., Interaction of NH_3 with aluminum nitride nanotube: electrostatic vs covalent. *Physica E*, 2011, **43**, 1717–1719.

Received 4 December 2014; revised accepted 1 March 2015